ACES Asian Chemical Editorial Society

doi.org/10.1002/asia.202200243

CHEMISTRY AN ASIAN JOURNAL Research Article

www.chemasianj.org

Tuning the Stereoselectivity of an Intramolecular Aldol Reaction by Precisely Modifying a Metal-Organic Framework Catalyst

Joel Cornelio and Shane G. Telfer*[a]

Abstract: We report the catalysis of an enantioselective, intramolecular aldol reaction accelerated by an organocatalyst embedded in a series of multicomponent metal-organic frameworks. By precisely programming the pore microenvironment around the site of catalysis, we show how important features of an intramolecular aldol reaction can be tuned, such as the substrate consumption, enantioselectivity, and degree of dehydration of the products. This tunability arises from non-covalent interactions between the reaction participants and modulator groups that occupy positions in the framework remote from the catalytic site. Further, the catalytic moiety can be switched form one framework linker to another. Deliberately building up microenvironments that can influence the outcome of reaction processes in this way is not possible in conventional homogenous catalysts but is reminiscent of enzymes.

Introduction

Porosity, crystallinity and the isoreticular principle are the bedrocks of metal-organic framework (MOF) chemistry.[1] From point of view of catalysis, porosity implies that reaction substrates can freely diffuse into the pores to interact with catalytic motifs and be transformed into products. Crystallinity aids in the precise design and characterization of the pore environment that will host the substrates. By leveraging the isoreticular principle, functional groups derived from molecular catalysts can be installed on ligands and introduced to MOFs without perturbing their topology. This has emerged as a powerful approach to the design of catalysts for many useful transformations.[2]

Most MOFs are made of one metal and one ligand. On the other hand, multicomponent MOFs such as MUF-7, MUF-77, and MUF-777 (MUF = Massey University Framework) are made up of three geometrically distinct linkers.[3] Two of these linkers are linear, ditopic linkers based on the 1,4-benzenedicarboxylate (bdc) and 4,4′-biphenyldicarboxylate (bpdc) skeletons. The third linker is a C_3-symmetric, tritopic tris(carboxylate) linker such as a hexaalkyltruxenetricarboxylate. All the linkers in multicomponent MOFs assume specific framework positions, which circumvents randomness and disorder. Since each of these linkers can be functionalised without perturbing framework assembly, programmed pores can be built up where the pore environments are precisely defined by a set of ligand functional groups. This enables the catalytic properties of these multicomponent MOFs to be tuned. We have shown that if one ligand bears a catalytic moiety, the other ligands can be armed with *modulators* to influence the catalytic process. This influence is transmitted by non-covalent interactions, which can tune the enantiomeric excess, selectivity and even the reaction pathway. Loose parallels can be drawn with the structural and functional properties of enzymes.[4] This combination of diversity and order is not encountered in traditional MOFs and other porous materials and their pore environments cannot be tuned with precision.

Previously, we reported the synthesis of MUF-77 frameworks with catalytic, (*S*)-prolinamide functionalised ditopic linkers and alkyl modulator groups installed on the truxene-based tritopic linker (Figure 1).[5] Using this material, we could control the kinetic behaviour and stereochemical outcome of the intermo-

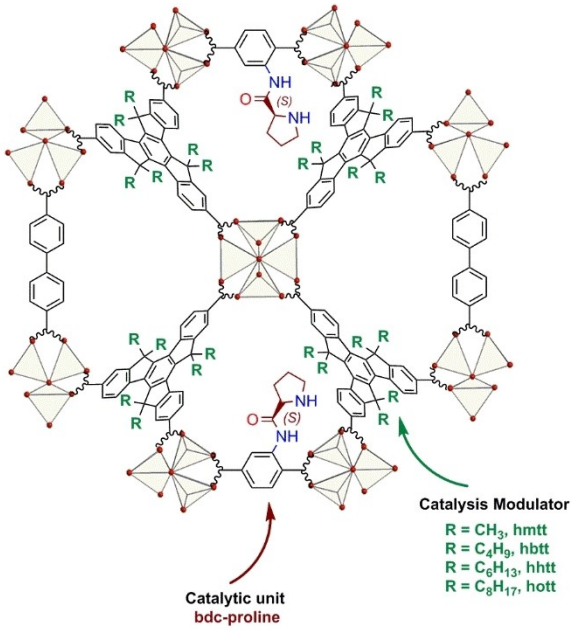

Figure 1. A schematic of a multicomponent MUF-77 framework with a bdc-proline catalytic group and alkyl 'modulators' (R) on the truxene linker.

[a] *Dr. J. Cornelio, Prof. S. G. Telfer*
School of Fundamental Sciences, MacDiarmid Institute of Advanced Materials and Nanotechnology
Massey University, 4410 Palmerston North (New Zealand)
E-mail: s.telfer@massey.ac.nz

Supporting information for this article is available on the WWW under https://doi.org/10.1002/asia.202200243

lecular aldol reaction of *p*-nitrobenzaldehyde and acetone. Small perturbations to the pore environment brought about by the alkyl modulator groups were able to override the inherent stereochemical preference of the catalyst group. Using the same frameworks, we were able to switch on a catalytic Henry reaction pathway with *m*-nitrobenzaldehyde and nitromethane, which is was not operative under homogeneous conditions.[6]

Here, we report on the way that MUF-77 catalysts can be tuned to influence an *intramolecular* aldol reaction. Substrate consumption, enantioselectivity, and the degree of dehydration of the products can all be influenced by functional groups installed at sites remote from the catalytic centre. Intramolecular reactions are well suited to porous catalysts since only one substrate needs to engage with the catalytic centre. This minimizes any potential mass transport limitations.[7] They typically have higher rate constants than their intermolecular counterparts, and often avoid the formation of multiple products or polymers.[8] Although, a vast number of organic transformations have been catalysed by MOFs, attempts to accelerate intramolecular reactions with MOFs are relatively fewer.[9] Reports of *asymmetric* intramolecular reactions catalysed by MOFs are especially rare.[10]

Results and Discussion

As a model reaction for intramolecular catalysis in MUF-77, we chose the exocyclisation of 1,6-hexanedial (**1**, Scheme 1), which produces 2-hydroxycyclopentane-1-carbaldehyde, **2**. Based on Baldwin's classification, the reaction is of the 5-*exo*-trig type.[11] This reaction can be catalysed by proline.[12] and by amine-terminal proline units in enzymes.[13] Compound **2** can spontaneously dehydrate to the achiral product, 1-formylclopentene, **3**. The rehydration of **3** to **2** has the potential to scramble the stereochemistry of **2**.

We first replicated the intramolecular aldol reaction of **1** using (*S*)-proline and (*R*)-proline as catalysts. To monitor the progress and kinetics of this reaction we used chiral gas chromatography. We were able to resolve the peaks for **1** and **3** and calibration curves were developed to enable their quantification (Figures S3 and S4). We could also resolve the peaks belonging to *anti*-**2** products but not those belonging to the *syn*-**2** products (Figure 2a, Figures S1 and S5).

From the chromatogram of the (*S*) and (*R*)-proline catalysed reactions, we made some additional key observations: **i)** *syn*-**2** products dehydrate faster than *anti*-**2** products (Figure S5a and S5b), and **ii)** When catalysed by (*S*)-proline, the *1R,2R* product

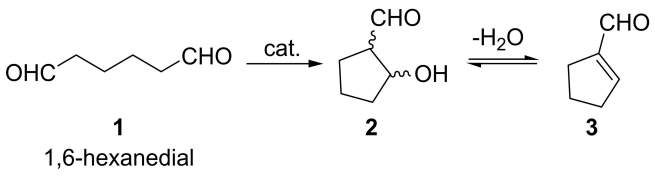

Scheme 1. The intramolecular aldol reaction of 1,6-hexanedial, **1**, to give 2-hydroxycyclopentane-1-carbaldehyde, **2**. Compound 2 can dehydrate to give the achiral compound 1-formylcyclopentene, **3**.

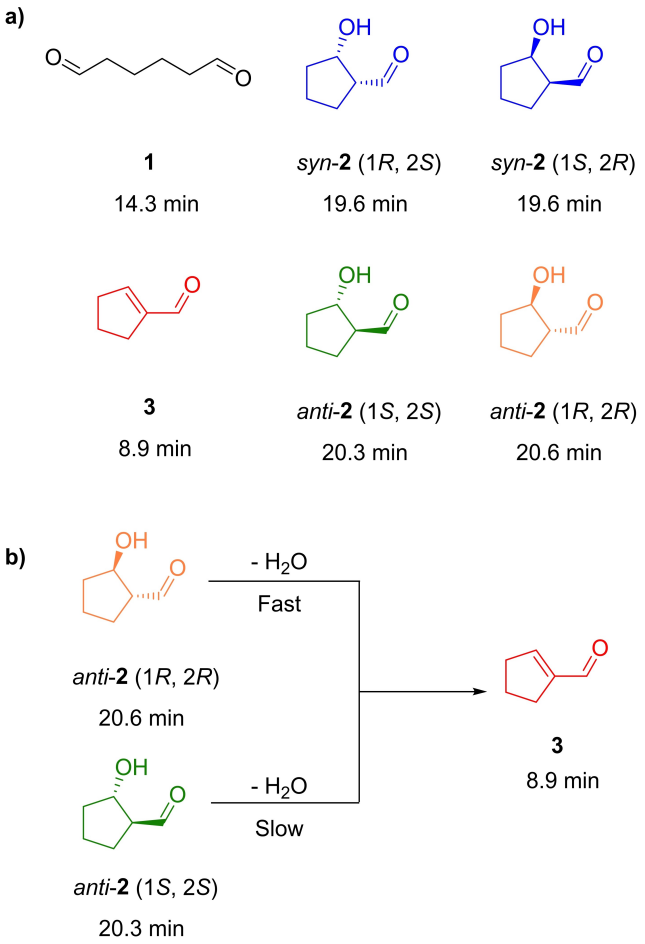

Figure 2. a) Structures of the substrate and products with their corresponding GC retention times (RT) when not derivatised. **b)** Differences in rates of dehydration of *anti* enantiomers brought about by catalysis with (*S*)-proline. The GC conditions are detailed in the ESI.

dehydrates faster than its *1S,2S* enantiomer (Figure 2b and S5a). The opposite pattern is seen for catalysis with (*R*)-proline (Figure S5b). The difference in the dehydration rate of enantiomers strongly implies that the chiral proline catalyst is an active participant in this reaction. This is consistent with the observed increase in the rate of dehydration when a higher loading of (*S*)-proline is used (Figure S6, Table S1). **iii)** The extent of the dehydration reaction influences the enantiomeric excess of the aldol products (Figures S7a and S7b). This indicates that dehydration is a reversible process. The achiral product, **3** undergoes conjugate addition of water to potentially give all four isomers of **2**, thus reducing the observed ee.[14] To design better stereoselective catalysts for the conversion of **1** to **2**, the degree of dehydration must be reduced.

To better resolve the peaks of *syn*-**2** in the gas chromatogram, we derivatised it with *N,O*-bis(trimethylsilyl)trifluoroacetamide (**4**, BSTFA, Scheme S1), which reacts quantitatively with the hydroxyl groups of **2** to give their more volatile trimethylsilylated products, **5**.[15] **4** does not react with aldehyde groups, and thus the unreacted substrate, **1**, and the dehydrated product, **3**, are undisturbed. As anticipated, the

chromatogram showed well resolved of peaks for all *syn* and *anti* products (Figure S2a), and the reported enantiomeric excess values were used for peak assignment.[12b] As expected, using (*R*)-proline as the catalyst inverts the distribution of enantiomers (Figure S2b).

Armed with this procedure, we replicated the reaction using $Me_2\boldsymbol{\alpha}$ and $Me_2\boldsymbol{\beta}$ as homogenous catalysts (Figure 3).[5–6] These esters are homogenous analogues of catalytic linkers that will subsequently be installed in the MOFs. To gauge their catalytic performance, we paid attention to four parameters: the substrate consumption, the percentage dehydration of the aldol products, and the enantiomeric excesses of the *syn* and *anti* products. To monitor all these parameters, the percentage consumption and dehydration were both calculated by collecting a gas chromatogram before derivatisation. Once derivatised with **4**, GC was performed again and the enantiomeric excess for the *syn* and *anti* isomers were calculated.

Reactions using $Me_2\boldsymbol{\alpha}$ and $Me_2\boldsymbol{\beta}$ consumed 42.4% and 17.2%, respectively, of **1** after 6 hours at 21 °C with a 10% catalyst loading (Table 1). These esters are slower catalysts than (*S*)-proline but produce similar or higher ee values in product **2**. We also performed kinetics experiments for the $Me_2\boldsymbol{\alpha}$ catalysed reaction by analysing the reaction mixture every 80 minutes.

By plotting the concentration of **1** with respect to time, we found that the consumption of **1** followed first-order kinetics with respect to **1** (Figure S8a). Tracking the concentration of **3** indicated that the dehydration reaction followed zero-order kinetics in **3** as a plot of peak area (RT = 8.9 min) versus time gave a straight line (Figure S8b). After 6 hours, the extent of dehydration was 6.5% which is extremely low compared to the extent of dehydration in the presence of (*S*)-proline. We propose that the free carboxylic acid group of proline may play a role in promoting dehydration through hydrogen bonding interactions with water.[16]

We then set about installing the catalytic linkers $\boldsymbol{\alpha}$ and $\boldsymbol{\beta}$ in multicomponent MOFs. We accomplished the synthesis of four MOF precatalysts with the $\boldsymbol{\alpha}$ linker via the solvothermal reaction of $H_2\boldsymbol{\alpha}$-Boc, H_2bpdc and H_3hxtt with $Zn(NO_3)_2$ in *N*,*N*-diethylformamide (Figure 4a).[5] These MOFs have the formula $[Zn_4O(hxtt)_{4/3}(bpdc)_{1/2}(\boldsymbol{\alpha}\text{-Boc})_{1/2}]$ where hxtt is a tritopic truxene-based linker with alkyl substituents of variable lengths.

To avoid its protonation and prevent coordination to zinc(II) ions during synthesis, the -NH group on the proline moiety was protected by a *tert*-butoxycarbonyl (boc) group.[17] Simple heating of the $[Zn_4O(hxtt)_{4/3}(bpdc)_{1/2}(\boldsymbol{\alpha}\text{-Boc})_{1/2}]$ precatalyst crystals under a dynamic vacuum at 200 °C for 20 hours removes the boc protecting groups in a clean thermolytic reaction (Figure 4b).[17a] This afforded four frameworks that are analogues of MUF-77 and

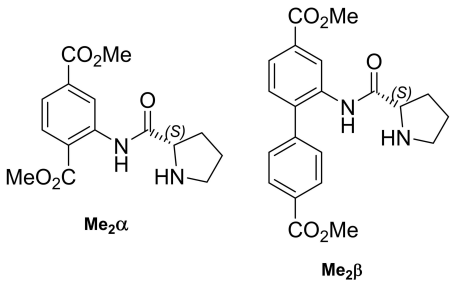

Figure 3. The structures of $Me_2\boldsymbol{\alpha}$ and $Me_2\boldsymbol{\beta}$ used as homogeneous catalysts used for the intramolecular aldol reaction of **1**.

Table 1. The intramolecular aldol reaction of **1** using homogenous catalysts.

Catalyst	% Consumption	% dehydration[a]	% ee[b] *anti*	*syn*
(S)-proline	>99	32.0	36.4	7.1
$Me_2\boldsymbol{\alpha}$	42.4	6.5	39.5	15.3
$Me_2\boldsymbol{\beta}$	17.2	16.9	44.0	8.7

Reactions performed at 21 °C with 10 mol% of catalyst with respect to 0.04 M 1,6-hexanedial in acetonitrile. [a] The ratio of peak area of **3** to sum of areas of **3** and all the isomers of **2**. [b] The ratio of difference in areas of peaks between the later eluting product and earlier eluting product relative to the sum of their areas.

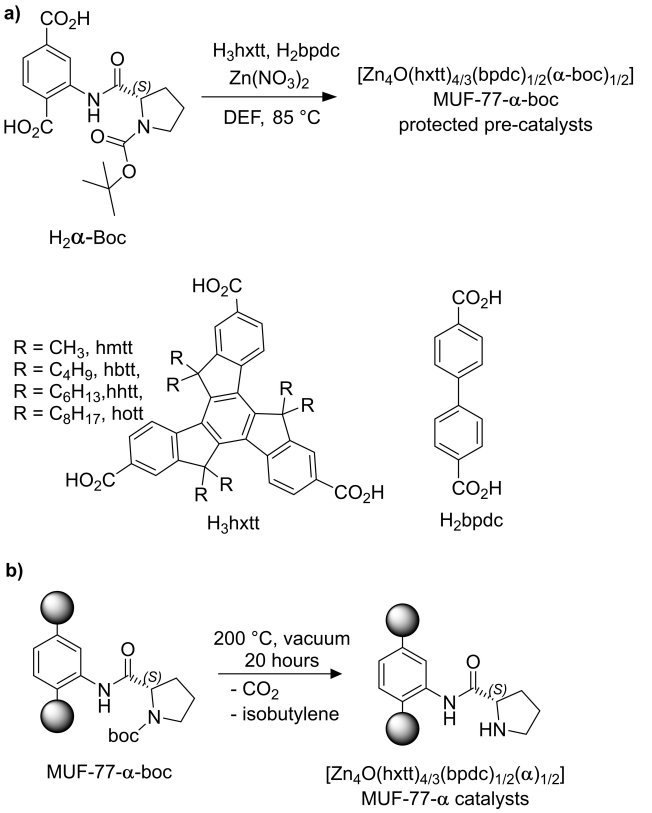

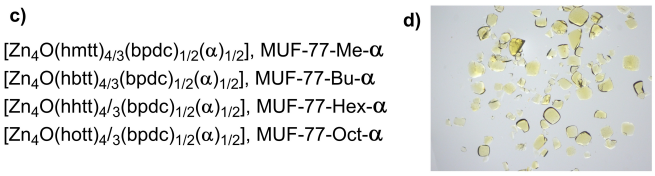

Figure 4. a) Solvothermal synthesis and deprotection of MUF-77-$\boldsymbol{\alpha}$ frameworks. The structures of the ligands are shown. **b)** Structure of the deprotected, catalytically active ligand in MUF-77-$\boldsymbol{\alpha}$ after thermolysis with the black circles representing $Zn_4O(COO)_6$ metal clusters. **c)** Formulae of MUF-77-$\boldsymbol{\alpha}$ frameworks obtained after thermolysis. **d)** Photos of the MUF-77-Oct-$\boldsymbol{\alpha}$ catalyst.

named MUF-77-X-α where X refers to the alkyl chain on the truxene linker (methyl, butyl, hexyl or octyl). Their phase purity was determined by PXRD measurements and was found to match the simulated PXRD pattern of MUF-77. This means that the formula for the catalytic MUF-77 frameworks is $[Zn_4O(hxtt)_{4/3}(bpdc)_{1/2}(\alpha)_{1/2}]$ as proven previously by ^{1}H NMR spectroscopy on acid digested samples.[5–6]

The MUF-77-X-α frameworks were used as catalysts for the intramolecular aldol reaction of **1**. Reactions were carried out using a mass of MUF-77-X-α that delivers 10 mol% of proline units (Table S2). This allows the results to be compared directly with the homogeneous reactions. The reaction products were quantified by GC. Analysis was first performed without BSTFA derivatisation to determine the amount of starting material that had been consumed and the degree of dehydration. The crystals were then removed using a syringe filter and the filtrate was treated with BSTFA and a second gas chromatogram was collected to calculate the ee. A series of control experiments were also performed. First, no catalyst was added, and the stock solution was let to stand for 6 hours at 21 °C. This control showed only a minor change in the peak area of **1** in the GC (Table 2, entry 7), which can be attributed to the oxidation of **1** to 6-oxohexanoic acid and adipic acid (Table S5). A second control was performed with $[Zn_4O(hott)_{4/3}(bpdc)_{1/2}(bdc)_{1/2}]$ which has no catalytic prolinamide group and therefore no reaction was observed (Table 2, entry 8). The third control was using the MUF-77-Oct-α-Boc precatalyst thus retaining the boc protecting group on the proline site, which showed no catalyst activity as expected (Table 2, entry 9).

These control experiments showed, **i)** that a deprotected proline group is required in the MOF to carry out the aldol transformation, **ii)** the reaction does not occur on the external surface or on any defect sites of the MOF, and **iii)** it is not catalysed solely by the modulator groups as MUF-77-Oct did not show any product peaks.

All the MUF-77-X-α catalysts show significantly increased catalytic activity compared to homogeneous Me_2α catalyst (Table 2, Entries 3–6). This demonstrates that the diffusion of **1** and **2** into and out of the framework is not a significant factor.

As the length of the alkyl chain on the truxene linker increases, differences in all parameters i.e. consumption, the degree of dehydration and % ee are seen (Table 2, Entries 3–6). These alkyl groups are located remote from the catalytic unit and are shown in the past to influence catalytic outcomes of intermolecular aldol and Henry reactions, and we can now extend this conclusion to intramolecular aldol reactions.[5–6] Their impact especially on the consumption and enantiomeric excess is quite remarkable.

The consumption of the substrate increases as the length of the alkyl chains increases, peaking at MUF-77-Hex-α and MUF-77-Oct-α. This increased activity counteracts the reduction in the framework pore volume that accompanies these alkyl substituents and shows that these modulator groups are effective as enhancing the catalytic process.

The ee of the *anti* products remain uniformly high across the series of catalysts and on par with the homogenous Me_2α. The *syn* products, however showed very low % ee ($< -5\%$). The earlier kinetic studies showed that the *syn* products dehydrate earlier and faster than the *anti* products. Their low ee value can therefore be ascribed to the reversible dehydration reaction of **2**.

Both MUF-77-Bu-α and MUF-77-Oct-α showed first-order kinetics for the consumption of **1** (Figure 5b). These kinetic profiles are similar to that of the homogenous catalyst Me_2α. This means that the mechanism for catalysis for Me_2α and MUF-77-α may be analogous.[18]

To gauge recyclability, we reused the crystals of MUF-77-Bu-α and MUF-77-Oct-α for catalysis. First, PXRD patterns of the MUF-77-X-α crystals were analysed before and after catalysis (Figure S9). The patterns were similar, indicating that the crystal structure was maintained throughout catalysis. Additionally, the crystals did not show any cracks when seen under a microscope (Figure 4c, S10). In the catalysis runs, we collected gas chromatograms (without derivatisation) every 80 minutes, helping us determine kinetic parameters (Table 3). No loss in catalytic activity was observed over multiple runs. After 400 minutes (6 hours and 40 minutes), the values obtained for consumption and degree of dehydration agreed with those obtained for the first catalysis run (Table S4). Additionally, the %

Table 2. Catalysis data for the intramolecular aldol reaction of **1**.

Entry	Catalyst	Ligand combination	Consumption [%]	% dehydration	% ee[a] *anti*	*syn*
1	(*S*)-proline	–	>99	32.0	36.4	7.1
2	Me_2α	–	42.4	6.5	39.5	15.3
3	MUF-77-Me-α	hmtt/bpdc/α	52.2	16.1	50.2	−0.3
4	MUF-77-Bu-α	hbtt/bpdc/α	72.9	29.5	35.9	−1.5
5	MUF-77-Hex-α	hhtt/bpdc/α	80.2	27.6	36.2	−0.7
6	MUF-77-Oct-α	hott/bpdc/α	80.6	55.7	25.3	−2.6
	Controls					
7	No catalyst	–	<2[b]	–	–	–
8	MUF-77-Oct	hott/bpdc/bdc	<2[b]	–	–	–
9	MUF-77-Oct-α-Boc	hott/bpdc/α-Boc	<2[b]	–	–	–

Notes: Reactions were performed in triplicate at 21 °C for six hours with 10 mol% of catalyst relative to **1**. [a] The ratio of difference in areas of peaks between the later eluting product and earlier eluting product to the sum of their areas. % dehydration is the ratio of peak area of **3** to sum of peak areas of **3** and all the isomers of **2**. Standard deviations are listed in Table S3. [b] Oxidised product seen, which was characterized by ESI-HRMS. Refer Table S4 for details.

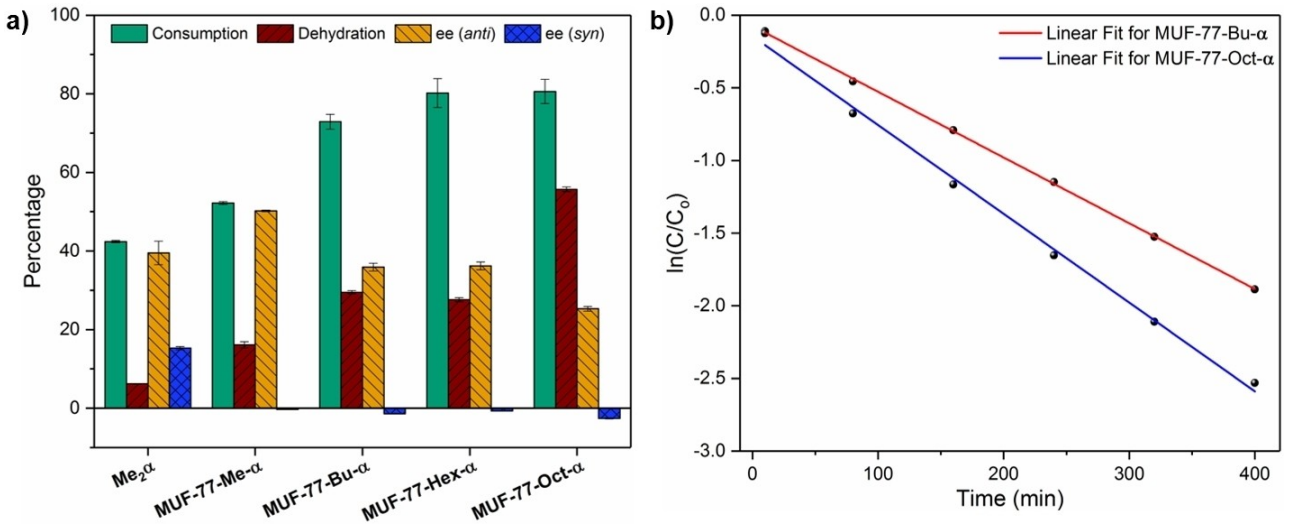

Figure 5. a) Comparison of heterogenous catalysis with different MUF-77-**α** systems with homogenous catalysis by Me_2**α**. The ligand combinations are shown along the horizontal axis. Experimental standard deviations are mentioned in Table S3. **b**) First-order kinetics for the consumption of **1** catalysed by MUF-77-Bu-**α** and MUF-77-Oct-**α** showing differences in their reaction rates. Here, C and C_o are concentrations of the substrate at the measured time and of the stock solution, respectively.

Table 3. Comparing rate constants for homogeneous versus MUF-77-α catalysed reactions.

Catalyst	Rate constant for consumption of 1 [min^{-1}]	Rate constant for dehydration [$mol\,L^{-1}\,min^{-1}$]
MUF-77-Bu-**α**	4.5×10^{-3}	2.6×10^{-5}
MUF-77-Oct-**α**	6.1×10^{-3}	5.7×10^{-5}
Me_2**α**	8.3×10^{-4}	2.7×10^{-6}

ee values for the *anti* products were also similar. This indicates that these MUF-77 catalysts are recyclable.

The rate constants between homogenous and heterogenous catalysts show major differences (Table 3). It is evident that both MUF-77-Bu-**α** and MUF-77-Oct-**α** catalysts fare better as catalysts for the intramolecular reaction than the homogenous catalyst, Me_2**α**. In fact, the rate constant for MUF-77-Oct-**α** is about 7.3 times higher than that of Me_2**α**. Although these rates are roughly similar for the MUF-77 catalysts, MUF-77-Oct-**α** dehydrates the product twice as fast as MUF-77-Bu-**α** (Figure S9). This is interesting, as both these catalysts contain the same active moiety, and have the comparable consumption rate constants, but very different rates of dehydration. The pore environments within these frameworks are different affecting the interplay between polar and steric effects, thus impacting H-bonding interactions between catalyst, substrate and dehydrated product.[19]

We also synthesised MUF-77-**β** frameworks with prolinyl groups attached to the bpdc linker (Figure 6a). This involved solvothermal synthesis and thermolysis of boc groups to give the catalyst, **β** (Figure 6b). We then replicated catalysis in similar conditions using 10 mol% of catalyst loading relative to **1** (Table S2), for the same time period. Once again, PXRD patterns before and after catalysis were identical (Figure S11) and photographs showed no cracks on the crystal surface (Figure S13).

The trends seen for these MUF-77-**β** catalysts are more complex (Figure 6d and Table S3). In all cases, their consumption of **1** is higher than that observed for Me_2**β**, indicating unhindered diffusion of the substrate into the MOF pores. The ee of the *anti* products is generally high, but dips for MUF-77-Oct-**β** (despite it showing the highest consumption). The dehydration of **2** varies in an unsystematic way across the series of catalysts.

For MUF-77-Bu-**β**, the *syn* product ee is higher than that for Me_2**β** (Table S3, entries 10 and 13). On the other hand, the *syn* products dehydrate more readily than the *anti* products and similar degrees of dehydration are observed for the reactions catalysed by MUF-77-Me-**α** and MUF-77-Hex-**β** (16.1% vs 15.8%; Table S3, entries 6 and 14). Despite this, the *syn* products show a higher ee when catalysed by MUF-77-Hex-**β**, indicating that the pore environment in this catalyst is better at stabilising *syn* products. The same can be said for MUF-77-Bu-**β**, for which the *syn* ee is 12.2%.

This stabilisation is confirmed further by comparing the diastereomeric ratios (d.r) between the different catalysts (Table 4). MUF-77-**α** catalysts produce more of the *anti* products when while MUF-77-**β** catalysts produce *syn* products in higher amounts. Such a reversal in the d.r. is not observed for homogenous catalysts Me_2**α** and Me_2**β** which have d.r. of 1.61 : 1 and 1.06 : 1, respectively. Similar reversals have been reported for intermolecular aldol reactions.[5,20]

The stereoselectivity of the enolexo cyclisation of **1** can be tuned by systematic modifications to multicomponent MOF catalysts. These modifications take the form of alkyl chains appended to the truxene-based framework linker. These chains decorate the pore environment that surrounds the site of catalysis and a host of noncovalent contacts can form with the

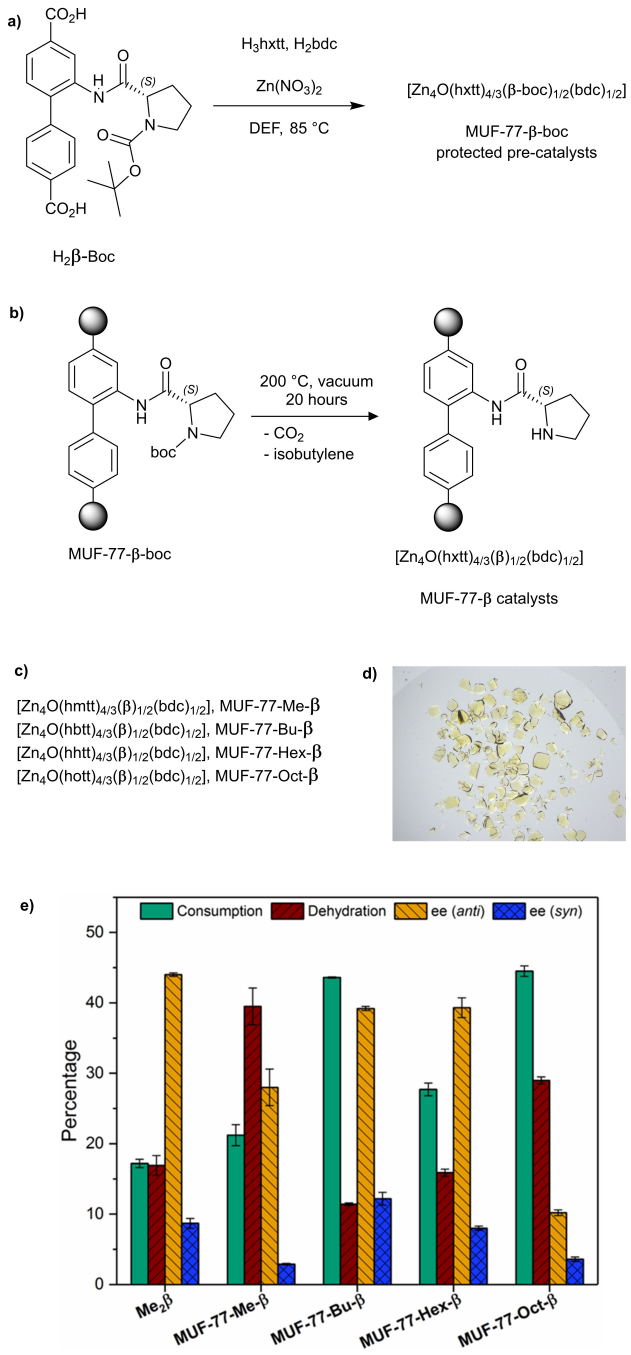

Figure 6. a) Solvothermal synthesis and deprotection of MUF-77-**β** frameworks, H_2bdc = 1,4-benzenedicarboxylic acid **b)** Structure of the deprotected, catalytically active ligand in MUF-77-**β** after thermolysis with the black circles representing $Zn_4O(COO)_6$ metal clusters. **c)** Formulae of MUF-77-**α** frameworks obtained after thermolysis. **d)** Photos of the MUF-77-Oct-**β** catalyst. e) Performance of MUF-77-**β** catalysts against its homogenous analogue Me_2**β**. Numerical values are reported in Table S3.

reaction substrate and intermediates (Figure 7). These contacts steer the outcome of the aldol reaction.[19] Specifically, the rate of consumption of the substrate (**1**) increases when the alkyl modulator groups are lengthened in the MUF-77-X-**α** catalysts. This is further aided by smaller pore volumes in these MOFs, effectively concentrating the reaction participants in the pore.

Table 4. Comparison of diastereomeric ratios for the aldol reaction of **1** catalysed by homogenous and heterogenous catalysts.

Catalyst	Ligand combination	d.r. *[syn:anti]*
(*S*)-proline	–	0.54 : 1
Me_2bdc-pro (Me_2**α**)	–	1.61 : 1
MUF-77-Me-**α**	hmtt/bpdc/**α**	0.71 : 1
MUF-77-Bu-**α**	hbtt/bpdc/**α**	0.77 : 1
MUF-77-Hex-**α**	hhtt/bpdc/**α**	0.84 : 1
MUF-77-Oct-**α**	hott/bpdc/**α**	0.71 : 1
Me_2bpdc-pro (Me_2**β**)	–	1.06 : 1
MUF-77-Me-**β**	hmtt/**β**/bdc	0.95 : 1
MUF-77-Bu- **β**	hbtt/**β**/bdc	1.31 : 1
MUF-77-Hex-**β**	hhtt/**β**/bdc	1.23 : 1
MUF-77-Oct-**β**	hott/**β**/bdc	1.42 : 1

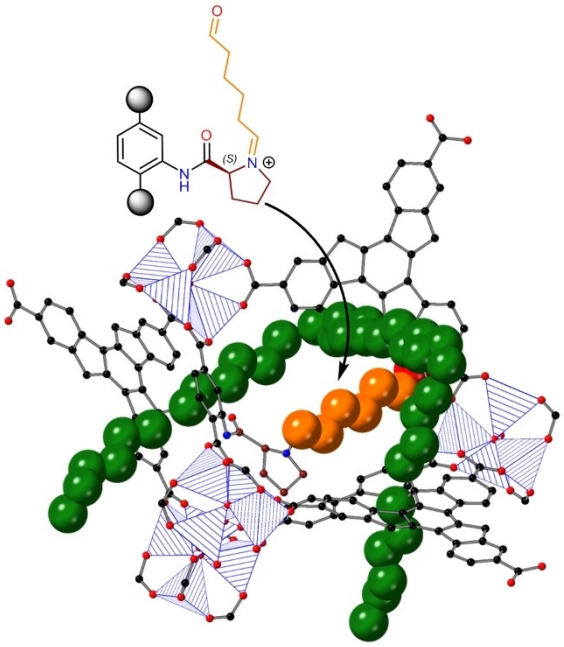

Figure 7. Schematic of a pore environment in MUF-77-Hex-**α** showing the substrate bound to the bdc-pro catalytic unit. The structure of the possible reaction intermediate is shown. The modulating hexyl groups are shown in green. Zn atoms are shown as striped tetrahedra, H atoms are omitted for clarity.

MUF-77-Me-**α**, on the other hand, has short methyl groups, is less able to influence the reaction and is less efficient as a catalyst. Being true single-site catalysts, correlations between the modulator groups and the catalytic activity can be determined with precision. Since a diverse array of catalytic and functional groups can be installed on this set of linkers, this approach is amenable to a wide array of challenging reactions and complex targets.

Conclusion

Intramolecular aldol reactions possess wide scope and applicability as C–C bond forming reactions.[21] Unfortunately, aldol products are prone to dehydration, which poses a significant

challenge and can lead to scrambling of the stereochemistry of the initially-formed cyclic aldol product.[22]

Via kinetics investigations, we show that programming the pores in MUF-77 can suppress their propensity of these aldol products for dehydration. This enhances the ee of the *syn* and *anti* stereoisomers of **1**. Additionally, the ease in making and characterising systematic modifications to the MUF-77-**α** and MUF-77-**β** catalysts contrasts with conventional catalysts and enzymes, where tuning the stereoselectivity of the aldol reactions requires extensive modifications of the catalyst. This in turn entails challenging synthetic chemistry or protein engineering processes.[44–46]

An intriguing feature of catalysis with MUF-77-**β** is the reversal in the enantioselectivity of *syn* product when compared to MUF-77-**α** catalysts. In homogenous media, examples for such reversal have been made for intramolecular aldol reactions when (*S*)-proline was replaced with (*S*)-homoproline.[23] In the MUF-77 catalysts presented here, a simple relocation of the same (*S*)-prolinamide catalytic moiety from one framework linker to another also reverses the selectivity. Related observations have been made for aldol reactions of *p*-nitrobenzaldehyde and acetone using other multicomponent MOF catalysts.[5]

The catalytic microenvironments in MUF-77 are pores that can be programmed pores by installing functional groups on the linkers. They are reminiscent of enzymes in that the modulator groups offer favourable non-covalent contacts with the reaction participants to the allow the reaction rate and steroselectivity to be tuned by functional groups remote from the catalytic site[24] and by switching position of the catalytic site in the framework.

Experimental Section

Experimental procedures, kinetic profiles, PXRD patterns, photographs and catalysis details.

Acknowledgements

We thank David Lun for assistance with gas chromatography. We are also grateful to the RSNZ Marsden Fund (Contract 14-MAU-024) and the MacDiarmid Institute of Advanced Materials and Nanotechnology for financial support. Open access publishing facilitated by Massey University, as part of the Wiley - Massey University agreement via the Council of Australian University Librarians.

Conflict of Interest

The authors declare no conflict of interest.

Data Availability Statement

The data that support the findings of this study are available from the corresponding author upon reasonable request.

Keywords: aldol reaction · heterogenous catalysis• intramolecular reactions · metal-organic frameworks · organocatalysis

[1] a) H. Furukawa, K. E. Cordova, M. O'Keeffe, O. M. Yaghi, *Science* **2013**, *341*, 1230444; b) Z. Ji, H. Wang, S. Canossa, S. Wuttke, O. M. Yaghi, *Adv. Funct. Mater.* **2020**, *30*, 2000238.
[2] a) H. Zhang, L.-L. Lou, K. Yu, S. Liu, *Small* **2021**, *17*, 2005686; b) X. Zhang, J. Han, J. Guo, Z. Tang, *Small Structures* **2021**, *2*, 2000141.
[3] a) L. Liu, K. Konstas, M. R. Hill, S. G. Telfer, *J. Am. Chem. Soc.* **2013**, *135*, 17731–17734; b) L. Liu, S. G. Telfer, *J. Am. Chem. Soc.* **2015**, *137*, 3901–3909; c) J. Cornelio, T. Y. Zhou, A. Alkas, S. G. Telfer, *J. Am. Chem. Soc.* **2018**, *140*, 15470–15476; d) A. Alkas, J. Cornelio, S. G. Telfer, *Chem. Asian J.* **2019**, *14*, 1167–1174.
[4] A. E. Platero-Prats, A. Mavrandonakis, J. Liu, Z. Chen, Z. Chen, Z. Li, A. A. Yakovenko, L. C. Gallington, J. T. Hupp, O. K. Farha, C. J. Cramer, K. W. Chapman, *J. Am. Chem. Soc.* **2021**, *143*, 20090–20094.
[5] L. Liu, T. Y. Zhou, S. G. Telfer, *J. Am. Chem. Soc.* **2017**, *139*, 13936–13943.
[6] T. Y. Zhou, B. Auer, S. J. Lee, S. G. Telfer, *J. Am. Chem. Soc.* **2019**, *141*, 1577–1582.
[7] B. A. Johnson, A. M. Beiler, B. D. McCarthy, S. Ott, *J. Am. Chem. Soc.* **2020**, *142*, 11941–11956.
[8] a) A. J. Kirby, M. Medeiros, J. R. Mora, P. S. M. Oliveira, A. Amer, N. H. Williams, F. Nome, *J. Org. Chem.* **2013**, *78*, 1343–1353; b) P. W. Mui, Y. Konishi, H. A. Scheraga, *J. Protein Chem.* **1986**, *5*, 29–49; c) T. C. Bruice, F. C. Lightstone, *Acc. Chem. Res.* **1999**, *32*, 127–136; d) M. L. Bender, M. C. Neveu, *J. Am. Chem. Soc.* **2002**, *80*, 5388–5391; e) A. R. P. Henderson, J. R. Kosowan, T. E. Wood, *Can. J. Chem.* **2017**, *95*, 483–504; f) S. Di Stefano, L. Mandolini, *Phys. Chem. Chem. Phys.* **2019**, *21*, 955–987.
[9] a) F. Vermoortele, M. Vandichel, B. Van de Voorde, R. Ameloot, M. Waroquier, V. Van Speybroeck, D. E. De Vos, *Angew. Chem. Int. Ed.* **2012**, *51*, 4887–4890; *Angew. Chem.* **2012**, *124*, 4971–4974; b) F. G. Cirujano, A. Leyva-Pérez, A. Corma, F. X. Llabrés i Xamena, *ChemCatChem* **2013**, *5*, 538–549; c) A. Dhakshinamoorthy, A. Santiago-Portillo, A. M. Asiri, H. Garcia, *ChemCatChem* **2019**, *11*, 899–923; d) B. Li, Z. Ju, M. Zhou, K. Su, D. Yuan, *Angew. Chem. Int. Ed.* **2019**, *58*, 7687–7691; *Angew. Chem.* **2019**, *131*, 7769–7773; e) P. Ji, X. Feng, P. Oliveres, Z. Li, A. Murakami, C. Wang, W. Lin, *J. Am. Chem. Soc.* **2019**, *141*, 14878–14888.
[10] T. Sawano, N. C. Thacker, Z. Lin, A. R. McIsaac, W. Lin, *J. Am. Chem. Soc.* **2015**, *137*, 12241–12248.
[11] a) J. E. Baldwin, *J. Chem. Soc. Chem. Commun.* **1976**, 734–736; b) K. Gilmore, R. K. Mohamed, I. V. Alabugin, *Wiley Interdiscip. Rev.: Comput. Mol. Sci.* **2016**, *6*, 487–514.
[12] a) C. Pidathala, L. Hoang, N. Vignola, B. List, *Angew. Chem. Int. Ed.* **2003**, *42*, 2785–2788; *Angew. Chem.* **2003**, *115*, 2891–2894; b) B. List, in *Modern Aldol Reactions*, **2004**, pp. 161–200.
[13] M. Rahimi, E. M. Geertsema, Y. Miao, J. Y. van der Meer, T. van den Bosch, P. de Haan, E. Zandvoort, G. J. Poelarends, *Org. Biomol. Chem.* **2017**, *15*, 2809–2816.
[14] E. Hartmann, D. J. Vyas, M. Oestreich, *Chem. Commun.* **2011**, *47*, 7917–7932.
[15] F. Orata, in: *Advanced Gas Chromatography - Progress in Agricultural, Biomedical and Industrial Applications* (Ed.: M. A. Mohd), InTech, **2012**, p. 470.
[16] a) G. Giubertoni, O. O. Sofronov, H. J. Bakker, *Commun. Chem.* **2020**, *3*, 84; b) B. Schobert, H. Tschesche, *Biochim. Biophys. Acta Gen. Subj.* **1978**, *541*, 270–277.
[17] a) D. J. Lun, G. I. Waterhouse, S. G. Telfer, *J. Am. Chem. Soc.* **2011**, *133*, 5806–5809; b) A. S. Gupta, R. K. Deshpande, L. Liu, G. I. N. Waterhouse, S. G. Telfer, *CrystEngComm* **2012**, *14*, 5701.
[18] P. H. Y. Cheong, K. N. Houk, *Synthesis* **2005**, *2005*, 1533–1537.
[19] L.-J. Yu, M. T. Blyth, M. L. Coote, *Top. Catal.* **2022**, *65*, 354.
[20] C. Kutzscher, G. Nickerl, I. Senkovska, V. Bon, S. Kaskel, *Chem. Mater.* **2016**, *28*, 2573–2580.

[21] a) S. J. Danishefsky, J. J. Masters, W. B. Young, J. T. Link, L. B. Snyder, T. V. Magee, D. K. Jung, R. C. A. Isaacs, W. G. Bornmann, C. A. Alaimo, C. A. Coburn, M. J. DiGrandi, *J. Am. Chem. Soc.* **1996**, *118*, 2843–2859; b) H. M. Lee, C. Nieto-Oberhuber, M. D. Shair, *J. Am. Chem. Soc.* **2008**, *130*, 16864–16866; c) D. Enders, O. Niemeier, L. Straver, *Synlett* **2006**, *2006*, 3399–3402; d) J. A. Abramite, T. Sammakia, *Org. Lett.* **2007**, *9*, 2103–2106.
[22] a) B. Liu, S. Wu, X. Yu, J. Guan, Q. Kan, *J. Colloid Interface Sci.* **2011**, *362*, 625–628; b) Y. H. Lam, K. N. Houk, *J. Am. Chem. Soc.* **2015**, *137*, 2116–2127.
[23] a) P. Buchschacher, J.-M. Cassal, A. Fürst, W. Meier, *Helv. Chim. Acta* **1977**, 60, 2747–2755; b) M. Limbach, *Tetrahedron Lett.* **2006**, *47*, 3843–3847.
[24] a) S.-I. Ozaki, T. Matsui, Y. Watanabe, *J. Am. Chem. Soc.* **1996**, *118*, 9784–9785; b) M. D. Toscano, K. J. Woycechowsky, D. Hilvert, *Angew. Chem. Int. Ed.* **2007**, *46*, 3212–3236; *Angew. Chem.* **2007**, *119*, 3274–3300.

Manuscript received: March 14, 2022
Revised manuscript received: March 30, 2022
Accepted manuscript online: April 25, 2022
Version of record online: May 23, 2022